Ann. Geophys., 29, 1873–1884, 2011
www.ann-geophys.net/29/1873/2011/
doi:10.5194/angeo-29-1873-2011

Annales Geophysicae

Observations of OI 557.7 nm nightglow at Kolhapur (17° N), India

N. Parihar[1], **S. Gurubaran**[2], **and G. K. Mukherjee**[3]

[1]Dr. K. S. Krishnan Geomagnetic Research Laboratory, Indian Institute of Geomagnetism, Allahabad 221 505, India
[2]Equatorial Geophysical Research Laboratory, Indian Institute of Geomagnetism, Tirunelveli 627 011, India
[3]Indian Institute of Geomagnetism, Navi Mumbai 410 218, India

Received: 2 November 2010 – Revised: 12 September 2011 – Accepted: 16 September 2011 – Published: 25 October 2011

Abstract. Ground-based nightglow observations of the atomic oxygen green line at 557.7 nm have been carried out at a low latitude station Kolhapur (17° N), India, during November 2003–April 2004 and December 2004–May 2005. The nocturnal behaviour of OI 557.7 nm intensity and a comparative study with simultaneous OH Meinel band temperature measurements has been presented. OI 557.7 nm intensity and OH temperature variations covary on many occasions. It was found that an 8 h tide characterizes the variation of intensity and temperature on most nights, and especially during the month of January. This is the first report of prolonged measurements of OI 557.7 nm emission from India.

Keywords. Atmospheric composition and structure (Airglow and aurora) – Meteorology and atmospheric dynamics (Middle atmosphere dynamics; Waves and tides)

1 Introduction

In the lower thermosphere, the absorption of solar ultraviolet radiation in Schumann-Runge bands, Herzberg continuum (at wavelengths 140–200 nm) and Lyman α line (121.5 nm) by molecular oxygen (O_2) results in its photodissociation, leading to the formation of atomic oxygen (O). A considerable amount of the atomic oxygen so produced then reaches the region in and around the upper mesosphere through downward transport. In the upper mesosphere, the photolysis of ozone (O_3) due to the solar radiation in the Hartley band (200–300 nm) acts as a complementary source of the atomic oxygen (O). The presence of atomic oxygen (O) in the mesosphere-lower thermosphere (MLT) region triggers a series of chemical reactions, and some among them are responsible for the nightglow phenomena (Brasseur and Solomon, 1984; Meriwether, 1989; Smith, 2004).

Nightglow emission due to the forbidden transition of atomic oxygen OI ($^1D_2 - {}^1S_0$) at 557.7 nm is one of the characteristic features of the spectrum of the terrestrial night sky, especially that originating in the MLT region. Several nightglow studies (McDade and Llewellyn, 1986; Bates, 1988, 1992, and references cited therein) indicate that at MLT heights, this emission is excited by the following two step energy transfer process (also called "Barth's excitation mechanism"):

$$O + O + M \rightarrow O_2^* + M \qquad \text{(a)}$$
$$O_2^* + O \rightarrow O_2 + O(^1S) \qquad \text{(b)}$$
$$O(^1S) \rightarrow O(^1D) + h\nu_{(557.7\,\text{nm})}$$

Here, O_2^* is an excited state of O_2, with the total excitation energy higher than the O (^{1}S) excitation energy. Recent advances in this area indicate that the excited state $c^1\Sigma_u^-$ of the molecular oxygen is the precursor for the emission of O (^{1}D) 557.7 nm line (see also Bates, 1992; and references cited therein). So far as the emission altitude is concerned, numerous in situ rocket-borne measurements as well as satellite observations (Yee and Abreu, 1987; Murtagh et al., 1990; Gobbi et al., 1992; Yee et al., 1997; Zhang and Shepherd, 1999) indicate the emission peak of this nightglow feature to be around 97 km.

Since the early observations of the spectrum of night sky by Rayleigh in 1922 (Rayleigh, 1924; Rayleigh and Jones, 1935), this emission has been extensively studied using ground-based nightglow photometry, in situ rocket experiments and space-borne spectroscopic observations with the objective of understanding the behaviour of the MLT region (especially its response to dynamics and transport processes). At the MLT heights, the dynamical forcings from the lower atmosphere (mainly gravity waves and tides) significantly control the atomic oxygen density; and OI 557.7 nm

Correspondence to: N. Parihar
(nparihar@iigs.iigm.res.in)

emission intensity, being directly dependent on atomic oxygen, is expected to reflect the dynamical influence in the form of temporal variations. Since the 1980s, Takahashi et al. (1977, 1985, 1989, 1998), Petitdidier and Teitelbaum (1977, 1979), Misawa and Takeuchi (1982), Yee and Abreu (1987), Oznovich et al. (1995), Shepherd and McLandress (1995), Zhang et al. (1998), Wiens et al. (1999), and Buriti et al. (2001) have reported the nocturnal behaviour of the oxygen green line emission. Fukuyama (1976), Petitdidier and Teitelbaum (1977), and Das and Sinha (2008) studied the effect of tidal dynamics on the intensity. Of late, Liu and Shepherd (2006) have reported the satellite measurements (WINDII instrument onboard UARS) of this nightglow feature. These authors found the multiple peaks in the emission profiles and attributed such features as a combined effect of gravity waves and tides. Most recently, Liu et al. (2008a, b) investigated the variations of this emission feature using the ground-based photometric data from Arecibo Observatory (Puerto Rico – 18° N, 67° W) and the satellite data from WINDII (on-board UARS).

Herein, the ground-based observations of OI 557.7 nm nightglow carried out at Kolhapur (17° N), India, are presented. Earlier, Chiplonkar and Tillu (1970), Rao and Kulkarni (1974), and Taori et al. (2003) have reported the observations of this emission feature from the Indian subcontinent, emphasizing the F-region contribution to the total intensity of the green line airglow. Kulkarni (1976) reported the nocturnal behaviour for a few nights using both rocket-borne instrumentation and ground-based photometric measurements near Thumba (8°33′ N), India. Mukherjee (2003) studied the small-scale gravity wave phenomenology (their horizontal phase speed, wavelength, and period) using an all-sky imager for a couple of nights at Panhala (17° N), India. However, the behaviour of this nightglow feature spanning a few months has not been reported till now from the Indian subcontinent. In this paper, the nocturnal behaviour of the green line of atomic oxygen during November 2003–April 2004 and December 2004–May 2005 is reported. Simultaneous observations of the OH spectroscopic temperature were available during the same period, and a comparative study of the two measurements has also been made. It is worthy to mention here that the observation epoch from November 2003 to April 2004 and December 2004 to May 2005 corresponded to the local winter and spring season; herein, a change in period of tide-like feature from December to March/April was noted.

2 Experimental set up, observation, and results

The nightglow observations of the green line of atomic oxygen at 557.7 nm (along with OH Meinel band emissions) have been carried out at Kolhapur (16.8° N, 74.2° E), India, on clear sky and moonless nights, centred on the new moon period using all-sky scanning photometers during November 2003 to April 2004 and December 2004 to May 2005. All-Sky Scanning photometers had a field of view of 7.25° and each of them utilized Burle C31034A GaAs photomultiplier tube (thermoelectrically cooled at −25 °C) for photon detection. During November 2003 to April 2004, a five-filter scanning photometer was operated along east-west direction from −30° to +30° zenith angle at equal angular spacing of 15°; and for the period between December 2004 and May 2005, a six-filter scanning photometer was operated along north-south direction from −30° to +30° zenith angle at equal angular spacing of 15°. The exposure time and delay time for each filter were so adjusted as to have a scan interval of ∼15 min. During each campaign, one filter was deployed for OI 557.7 nm observations and two filters were used for OH Meinel band measurements. During the November 2003 to April 2004 epoch, the P_1 (3) line and integrated R-branch of OH (7, 2) Meinel band was monitored; whereas the intensity measurement of the P_1 (2) and P_1 (4) line of OH (6, 2) Meinel band was made during December 2004 to May 2005 epoch. Also, the corresponding background emission was measured separately. The details of the optical filters used in the present study are presented in Table 1. The corrections due to the photomultiplier dark current, the response of photomultiplier towards a particular wavelength, and the transparency of filters were incorporated in the collected nightglow data. On most of the occasions, the signal-to-noise ratio was better than 70. In intensity data, the maximum uncertainty in OI 557.7 nm and OH (6, 2) Meinel band intensity measurements was 9 %, whereas OH (7, 2) Meinel band intensity values were uncertain by 16 % or less. The authors understand that the calibration is very important; however, due to non-availability of a standard source of light, the observed intensities were not calibrated in Rayleigh. Efforts are underway to procure a secondary source (utilizing MgO coated screen illuminated by a standard tungsten ribbon lamp of known spectral output) for calibration, and in future the measurements will be presented on an absolute Rayleigh scale. The spectroscopic OH rotational temperatures (a proxy of atmospheric temperatures near 87 km) were retrieved from the OH Meinel band intensities (see Parihar and Mukherjee, 2008, for details of the method of OH temperature retrieval from the knowledge of intensity). Some results of the OH nightglow measurements have been published by Parihar and Mukherjee (2008). In this report, the results of OI 557.7 nm nightglow observations and comparison of OI 557.7 nm and OH temperatures are presented. The nightglow data of nights for which the observations were made for 6 h or more have been considered for the present study, and those nights contaminated with the high level of moonlight and the presence of clouds were ignored. Complying with these criteria, forty-nine nights of useful observations were available for meaningful study. For the entire period of observation, the geomagnetic activity index (Ap) varied between 2 and 87, whereas the solar F10.7 cm flux lay in the range 82–178. Although the observations involved

off-zenith measurements as well, the results of only zenith measurements are presented here for simplicity.

2.1 Nocturnal behaviour of OI 557.7 nm emission

Some typical examples of the nocturnal variation (in IST) of OI 557.7 nm emission intensity are shown in Fig. 1. The intensity values of an individual dataset were divided by the nighttime mean value to obtain a normalized time series, and the normalized intensity variations are presented in the plots. The topmost-left panel represents the nocturnal variation of the intensity averaged over the entire observation epoch. On most of the nights shown in Fig. 1, the intensity is observed to maximize between 20:00 h and 22:00 h as compared with the rest of the night, and a decrease of intensity from the evening hours to midnight can clearly be seen. Often, the intensity was found to increase after midnight: the variations observed on 29–30 November 2003, 22–23 December 2003, 23–24, 25–26 January 2004, 19–20 February 2004, and 9–10 February 2005 represent a few good examples of such post-midnight increases. Such variations were sometimes marked by the occurrence of the midnight minimum of intensity between 00:00 h and 02:00 h (e.g. 18–19 April 2004). This nocturnal feature is presented in detail in succeeding paragraphs. On many occasions, the monotonous decrease of intensity continued throughout the night, and the nocturnal variation of 10–11 March 2005 represents a typical example of such trend. On such nights, the variation of OH Meinel band intensity also showed similar tendency (Parihar and Mukherjee, 2008). This type of nocturnal variation is a widely observed feature, and has been explained in terms of the loss of atomic oxygen and absence of photolysis during the night (Takahashi et al., 1977). Sometimes such monotonous decreasing tendency was superseded by an increase in intensity during the dawn hours. On the night of 14–15 February 2004, 18–19 February 2004, and 17–18 April 2004, a decrease of intensity from evening followed by an increase of intensity during dawn hours can be observed. Such an increase of intensity during morning hours has also been reported by Takahashi et al. (1989). Moreover, the intensity remained fairly constant after midnight on few occasions (e.g. 10–11 April 2005). Such behaviour is also noticeable in the average trend of the nighttime variation of intensity. On the night of 5–6 April 2005, the oscillatory features superimposed over a constant trend were seen. A glance at Fig. 1 also reveals that the intensity variations were sometimes smooth (e.g. ∼29–30 November 2003, 18–19 February 2004, 19–20 February 2004, 18–19 April 2004, 9–10 February 2005 and 10–11 April 2005) as well as were highly perturbed (e.g. ∼18–19 December 2003, 14–15 February 2004, and 5–6 April 2005). Such perturbed variations in intensity have been attributed to the changes in the temperature and local concentration of the reacting species caused by gravity waves (Takahashi et al., 1979). Often, short period oscillations superimposed over the nighttime trend were observed, and the variations observed on 29–30 November 2003, 22–23 December 2003, 18–19, and 19–20 February 2004 represent a few examples of this trait. In summary, two types of nocturnal trends were more frequent: firstly, a decrease of intensity from evening to dawn hours; and secondly, the decrease of intensity from pre-midnight to midnight hours, thereby attaining a minima around 01:00 h followed by the post-midnight increase. Although it is not very convincing, the latter feature can also be observed as a shallow dip in the plot of averaged nocturnal variation in Fig. 1 (topmost left). The occurrence frequency of monotonous decrease of intensity was about 45 %, whereas the midnight minimum of intensity was observed on approximately 43 % of nights. On the rest of nights, a constant trend with superimposed small wave-like variations was observed. The OH intensity measurements carried out during the same period show a similar nocturnal behaviour. In OH intensity measurements, the steady decrease of intensity from evening to dawn hours was present on nearly 51 % of nights, whereas approximately 31 % of the nights were noticed to have the midnight minimum of intensity (Parihar and Mukherjee, 2008).

Some examples of the nocturnal behaviour of OI 557.7 nm emission featuring the midnight minimum of intensity are presented in Fig. 2 (top row). An investigation of the entire OI 557.7 nm database characterized by such feature indicates that the intensity was comparatively more between 20:00 h and 22:00 h, and the minimum occurred between 00:00 h and 02:00 h. This is clearly noticeable from the plots shown in Fig. 2, as well as from a few plots of Fig. 1 (viz. 29–30 November 2003, 22–23 December 2003, 23–24, 25–26 January 2004, 19–20 February 2004 and 9–10 February 2005). Yee and Abreu (1987) have reported very similar nocturnal behaviour of this emission feature. Using the photometric measurements of OI 557.7 nm emission made by Visible Airglow Experiment (VAE) onboard the Atmosphere Explorer satellite, they investigated this feature and found a strong maximum of intensity during post-sunset hours (∼21:00 h), followed by post-midnight minimum near 02:00 h (notably in the Northern Hemisphere). Takahashi et al. (1985) noted the pre-midnight peak to occur around 22:30 h. Brenton and Silverman (1970) analysed the diurnal variation of this emission for 22 stations and found the diurnal variability to exhibit a pronounced minimum during the night at a few stations. Kulkarni (1976) presented a few nights of OI 557.7 nm emission from Thumba (8°33′ N), India, wherein the minimum intensity was observed between 23:00 h and 02:00 h followed by an increase thereafter. Recently, Liu et al. (2008b) observed the nocturnal behaviour of this emission feature to exhibit minimum and maximum, and found the emission to be larger in the early morning hours than in the early night. Several other investigators have reported this type of nocturnal variation of OI 557.7 nm intensity (Takahashi et al., 1977, 1989, 1998; Petitdidier and Teitelbaum, 1979; Oznovich et al., 1995; Shepherd and McLandress, 1995; Zhang et al., 1998; Wiens et al., 1999; Buriti et al., 2001). Although the

Table 1. Characteristics of the optical filters used for the nightglow observations at Kolhapur during November 2003 to April 2004 and December 2004 to May 2005.

Observation epoch	Nightglow emission (wavelength in nm)	Optical filter deployed		Transparency (%)
		Central wavelength in nm	Bandwidth (fwhm) in nm	
November 2003–April 2004	OI 557.7 nm	557.80	0.88	57
	P_1 (3) line of OH (7, 2) band	692.68	0.40	45
	R-branch of OH (7, 2) band	683.35	2.80	66
	Background continuum	530.00	1.80	58
December 2004–May 2005	OI 557.7 nm	557.80	0.88	57
	P_1 (2) line of OH (6, 2) band	840.10	0.80	65
	P_1 (4) line of OH (6, 2) band	846.70	0.90	55
	Background continuum	857.00	2.00	53

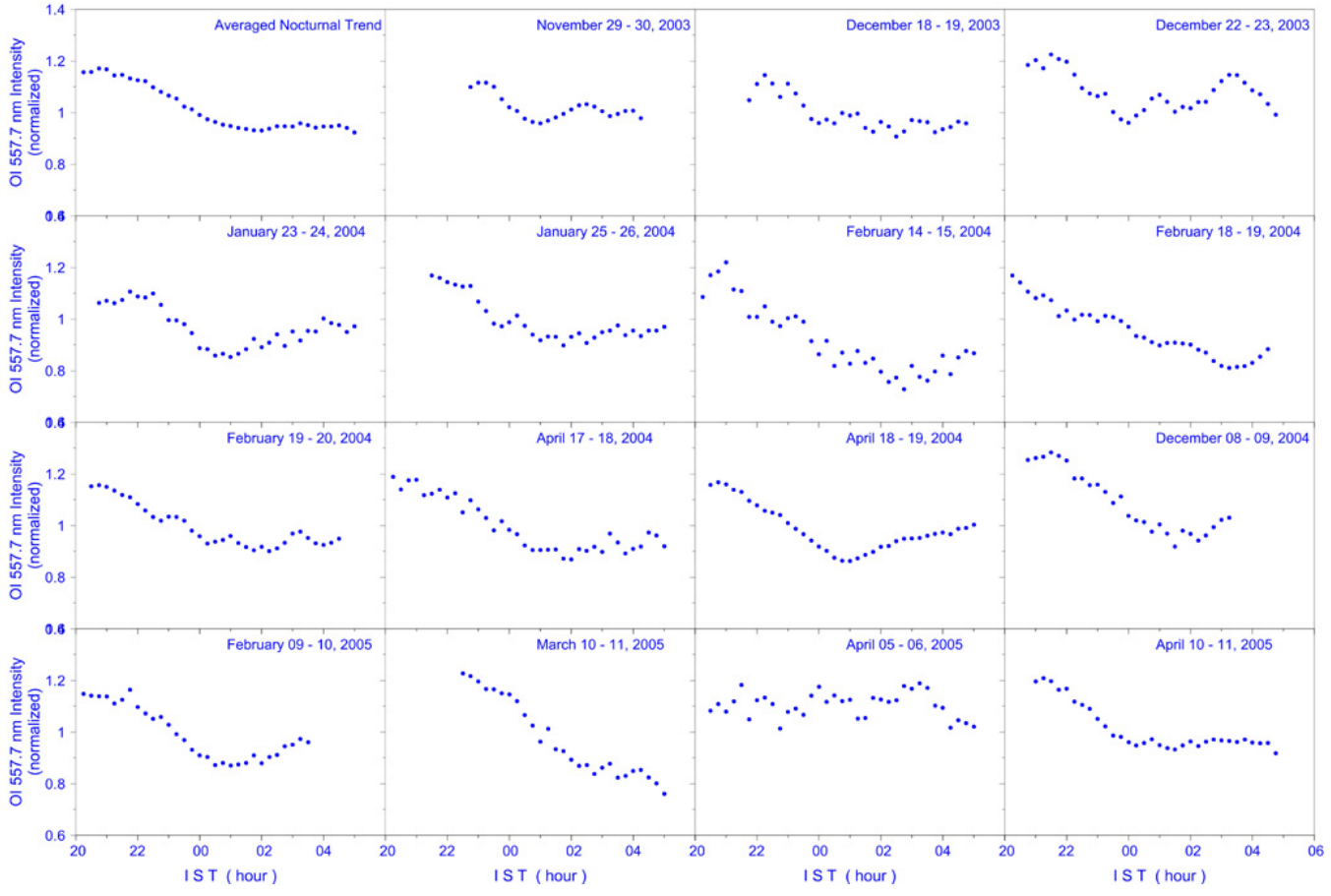

Fig. 1. Nocturnal variation (in IST) of OI 557.7 nm emission intensity at Kolhapur.

earlier measurements correspond to different epochs and locations on the globe, it is interesting to note that the occurrence of minima noticed here is in par with earlier reports, and this speaks of the general behaviour of this emission feature globally during night. It is now well known that such observed variations of intensity are mainly due to the changes in the local density of atomic oxygen. Takahashi et al. (1977, 1998), Petitdidier and Teitelbaum (1979), and Yee and Abreu (1987) have accounted for such an observed feature to an increase in atomic oxygen density in the post-midnight period, explaining that such a phenomenon would happen either as a consequence of an increase of mixing ratio or a change in

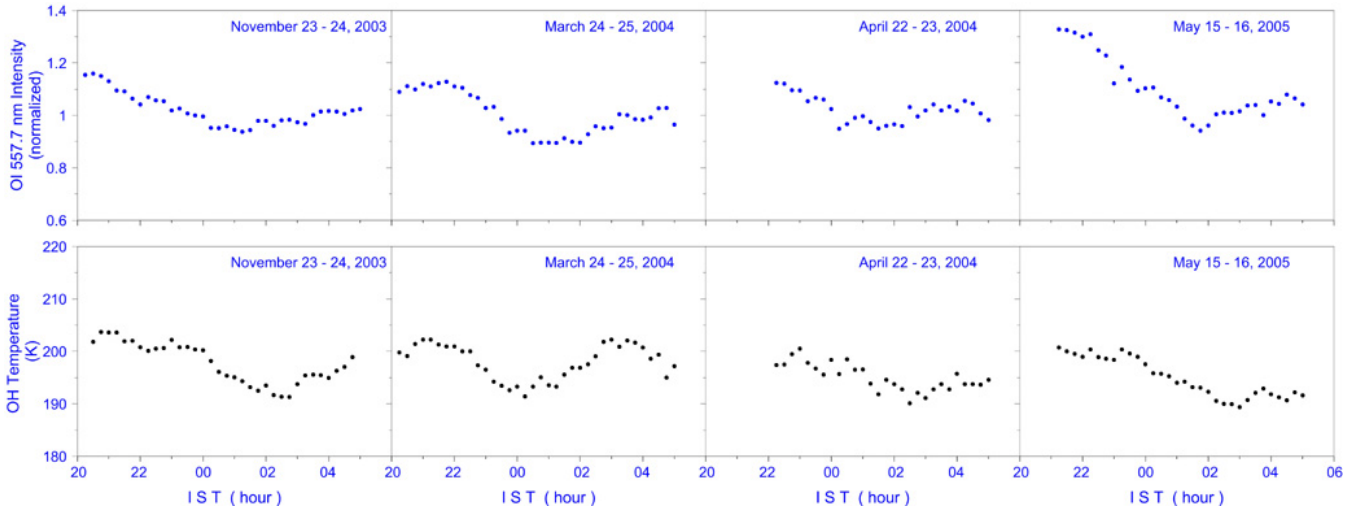

Fig. 2. Examples of the nocturnal trend of OI 557.7 nm emission featuring the midnight minimum of intensity (top row). The nocturnal variation of the OH temperature on the corresponding night is shown in the bottom row.

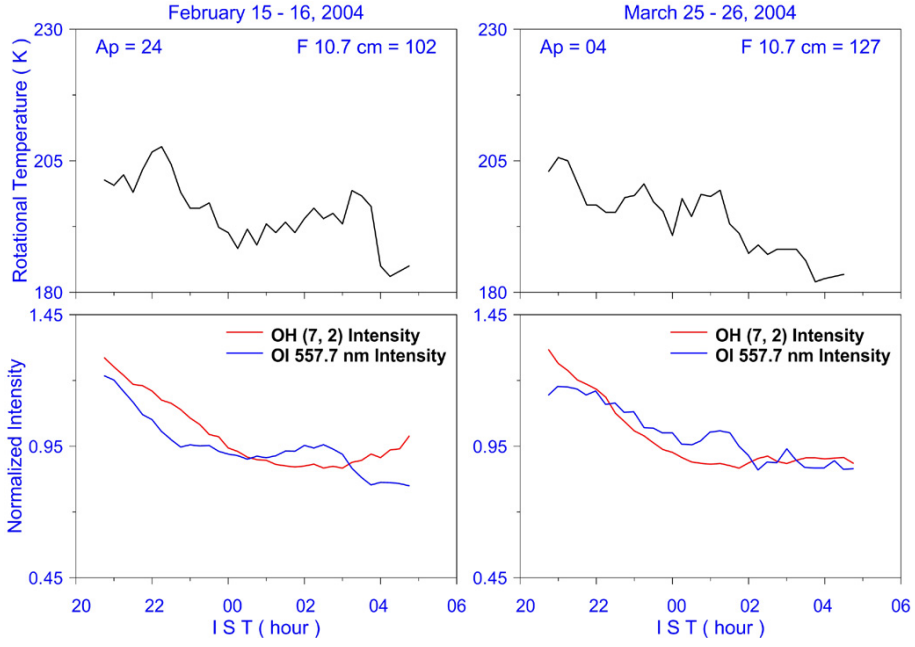

Fig. 3. Simultaneous observations nocturnal variations of OI 557.7 nm emission, OH Meinel band and the derived OH temperatures (the variation of OH temperature on the night of 15–16 February 2004 has already been reported by Parihar and Mukherjee, 2008).

atmospheric density and temperature around 97 km by the atmospheric tidal motions.

On such nights, the nocturnal variation of OH rotational temperature showed a similar trend. The bottom row of Fig. 2 depicts the variation of OH temperature on the corresponding night. A close resemblance in the nocturnal variation between the two measurements with a phase difference (∼1 h) can clearly be seen. Some examples of OI 557.7 nm and OH intensity variations, and OH temperature variations are shown in Fig. 3. Herein, OH emission intensity represents the sum of intensities of OH nightglow features that were observed (i.e. P_1 (3) line and the integrated R-branch for OH (7, 2) Meinel band measurements, and P_1 (2) and P_1 (4) lines for OH (6, 2) Meinel band observations). On the night of 15–16 February 2004, a decrease of intensities and temperature until local midnight and then a slight increase afterwards can be observed. A long period tide-like signature can clearly be seen in temperature variation (in addition to the short period fluctuations induced by gravity waves); however, the same effect is less pronounced in the intensity

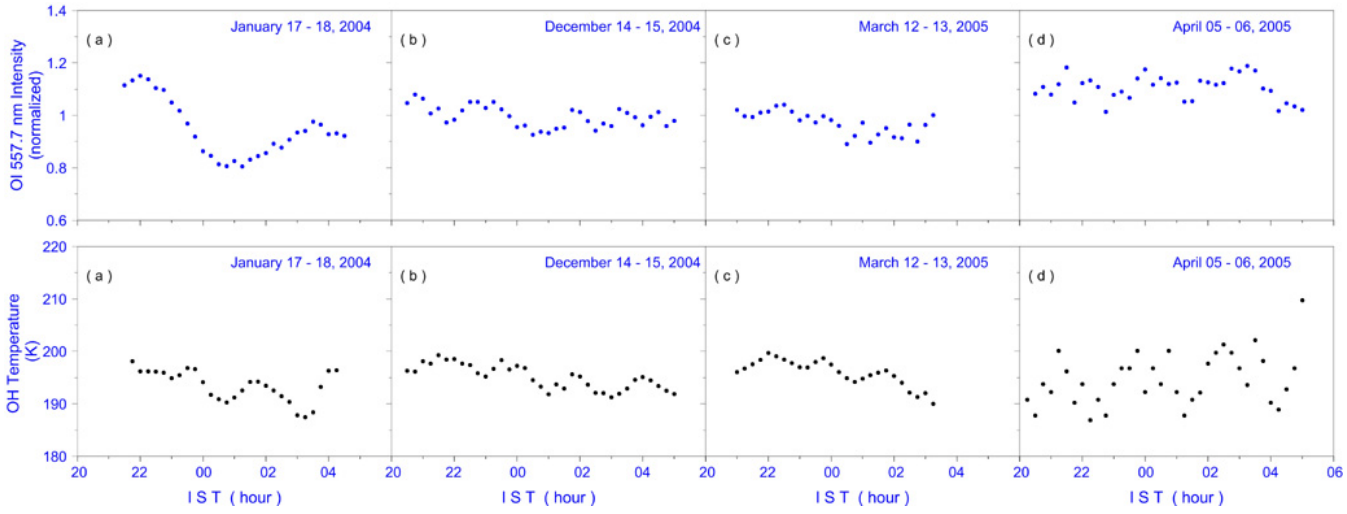

Fig. 4. Examples of gravity wave induced variations in OI 557.7 nm intensity (top row) and the OH temperature (bottom row).

variations. A correlation analysis indicates that the variation of OI 557.7 nm leads that of the OH (7, 2) band by about 1 h. Sometimes a correlated decrease of two intensities as well as OH temperature was observed from the beginning of the night to dawn hours (for example ∼ the variations observed on 25–26 March 2004), and this covariation improved on longer time scales. On most occasions, OH temperature variations were highly correlated with the OH intensity variations (Parihar and Mukherjee, 2008). A detailed discussion of the observed dynamical features in OI 557.7 nm intensity and OH temperature data is presented in the succeeding section.

2.2 Dynamical signatures observed in OI 557.7 nm intensity and OH temperature data

Gravity waves and tides strongly influence the temperature field of the MLT region and the nocturnal behaviour of the emissions from this region – in time-scales ranging from few minutes to a day. According to Takahashi et al. (1979), the mechanisms that contribute to the nocturnal variations of any emission feature from the upper mesosphere-lower thermosphere region are: firstly, a change in photochemical equilibrium, resulting in a change of mixing ratios of the atomic constituent involved; secondly, a variation in turbulence, resulting in enhancement of the eddy diffusion which in turn is responsible for the transport of minor species specially atomic oxygen; and thirdly, a change in the density of reacting species and the ambient temperature induced by the propagation of gravity waves and atmospheric tides. The alterations that are produced in turn affect the rate of the airglow producing photochemical reaction, and the changes sharply appear as variations in airglow intensity. Nocturnal variability observed in the plots of Figs. 1, 2, and 3 clearly reveal the presence of short-term (∼1–3 h) as well as long period (8 h or more) oscillations. In order to identify the oscillations present in the intensity and temperature data, Correlation (autocorrelation as well as cross-correlation) and Lomb-Scargle Analysis of the intensity and temperature series were performed and the results are presented below. Assuming that the OH and OI 557.7 nm emission peak is located at 87 km and 97 km, respectively, and remain unchanged during the night, the phase speed and vertical wavelength of the wave that was observed at both layers have been estimated (Takahashi et al., 1985, 1998). As the dataset for individual months was sparse and broken in nature, no attempt was made to study the planetary wave signatures.

2.2.1 Gravity wave induced short period oscillations

Herein, the wave events of less than 6 h have been considered. Some examples of these gravity wave induced variations in OI 557.7 nm intensity (top row) and OH temperature (bottom row) are shown in Fig. 4. On a few nights, OI 557.7 nm emission layer appeared to be steady in context to the short-period oscillations; however, the same was not observed in the OH layer on those nights. Often the waves that were observed in the OH emission layer were not present at OI 557.7 heights, and most likely these waves dissipated below OI 557.7 emission peak during the course of their propagation. Plots in panel (a) of Fig. 4 represent a typical example of such an event on the night of 17–18 January 2004. Simultaneous measurements of OI 557.7 nm nightglow and OH temperature have been reported by Cogger et al. (1988), wherein the authors noticed this feature (i.e. the presence of short-period oscillations in the temperature series and not in OI 557.7 nm data series) on a few occasions. On the whole, the OH temperature variations (∼19 %) were larger than those of OI 557.7 nm intensity (viz. ∼11 %). However, there were nights wherein similar waves were noted in OH

temperature and OI 557.7 nm intensity dataset. For example, on 25–26 March 2004 (shown in right panel of Fig. 3), a 2.1 h wave (having phase speed of 10 km h^{-1} and vertical wavelength of 21 km) was noted in both the datasets. On 14–15 December 2004 (shown in panel (b) of Fig. 4), a wave of periodicity of 2.2 h, phase speed of 13.3 km h^{-1} and vertical wavelength of 29.3 km was common at both the layers. Sometimes several similar waves were observed at both layers on a single night. For example, on 12–13 March 2005 (panel (c) of Fig. 4), the waves having period of 2 and 3 h were observed in both the layers. Plots in the panel (d) of Fig. 4 represent an event in which a 2.7 h wave (having phase speed of 24 km h^{-1} and vertical wavelength of 64 km) was noted in both the layers. Lomb-Scargle analysis of the entire database suggests the dominance of a wave of period 2.5 h and 2.6 h in OH temperature and OI 557.7 nm intensity dataset, respectively. Similar observations have been reported by Cogger et al. (1988). The authors found in most cases similar wave structures in green line intensity and OH temperature.

It is well known that the rate of most of the chemical reactions (especially those involving members of O_x and HO_x families) depend upon the temperature of the surrounding atmosphere; hence, a significantly correlated behaviour of OI 557.7 nm intensity and OH temperature is expected (Takahashi et al., 1979). Clemesha et al. (1991) analyzed a large database of the upper mesospheric nightglow features (OH band, O_2 atmospheric band, and OI 557.7 nm emission, and the derived spectroscopic temperatures). The authors found the nightly mean intensities to be highly correlated with the nightly mean OH temperatures, and attributed this to the correlated temperature and density changes in the upper atmosphere. In order to investigate the temperature dependence of OI 557.7 nm intensity, the 3 h averaging of the entire intensity and temperature dataset was performed. A window of 3 h was preferred because the periodicity of most of the short period waves observed was less than 3 h. The correlation and regression analysis of this averaged intensity and temperature database was performed. Though the correlation analysis suggests a weak dependence of the intensity on the temperature, the regression analysis does not indicate any relationship of the two quantities.

2.2.2 Tide-like long period oscillations

In the plots of Figs. 1, 2, and 3, the clear signatures of long period oscillation can be seen with the well defined minima of intensity and temperature. For example, on the night of 22–23 December 2003, 23–24 January 2004, 24–25 March 2005, two distinct peaks can clearly be seen – one around 21:45 h and another one around 03:45 h. A well defined crest and trough is evident in the majority of nocturnal variations. It is now well known that solar tides dominantly control the long term variations observed in the MLT region nightglow emissions through the downward transport of atomic oxygen from the lower thermosphere. These atmospheric oscillations arise due to the absorption of solar radiation by tropospheric water vapour, and the stratospheric and mesospheric ozone, and have periodicities of a solar day and its sub-harmonics (i.e. 24, 12, 8, 6, 4.8, 4 h, etc.). Specifically with reference to OI 557.7 nm emission, for example, Fukuyama (1976) reported the presence of the semidiurnal variation in its intensity at mid-latitude and interpreted it as an influence of solar semidiurnal tide. The Lomb-Scargle analysis of the dataset of individual months indicates the presence of diurnal, semidiurnal, as well as terdiurnal tidal components. Table 2 tabulates the results of this analysis for each month. In the table, the first dominant component is inscribed in bold-underlined, and the second one by bold letters only. A glance at the table clearly indicates that the results of two datasets greatly complement each other. A transition of observed harmonics from December to March can be noted from Table 2: $\sim$ firstly, the semidiurnal tide governs the observed variations during December; secondly, the terdiurnal feature explicitly dominates during January; and thirdly, the variations during February are mainly controlled by semidiurnal tide (with minor contribution from diurnal and terdiurnal components), whereas a mixture of semidiurnal and terdiurnal tides characterize the variation during March. In the Indian subcontinent, January marks the peak winter month. Herein, firstly a migration of dominant feature from semidiurnal to terdiurnal tide takes place during December and January, and then a migration of dominant feature from terdiurnal to semidiurnal component can be seen during January and February. During March–May, both the semidiurnal and diurnal features were equally present. Some examples of these observed features are presented in Fig. 5 (with OI 557.7 nm intensity variations in the left column and OH temperatures in the right column). Based on Lomb-Scargle analysis, a sinusoidal least square fit (confidence level of 95 %) of the form $A\sin[(2\pi/T)(t-\phi)]$ was applied to the data, and is represented by the solid curve in the plots of Fig. 5. A high-quality correspondence between the observed variations of quantities, viz. OI 557.7 nm emission intensity and temperature and the forced tidal harmonic fit can clearly be seen. This indicates that the variations are probably driven by the corresponding tidal wave – an important dynamical feature of the MLT region.

Statistically, the 8 h feature was the most occurring long-period oscillation, and was observed during the spring months well apart from the peak winter month of January. Apart from the Lomb-Scargle analysis and correlation analysis, a careful visual inspection of the individual intensity and temperature plots of the entire database also indicates the frequent occurrence of the 8 h feature. Generally, a crest and a trough in the intensity variation appear around $\sim$21:00 h and $\sim$01:00 h, respectively, thereby suggesting a wave of periodicity $\sim$8 h. On such nights, OI 557.7 nm intensity variation leads OH temperature variation by about 1 h. As the month of January was distinctly characterized by the 8 h feature, an averaging of the normalized nocturnal variations was

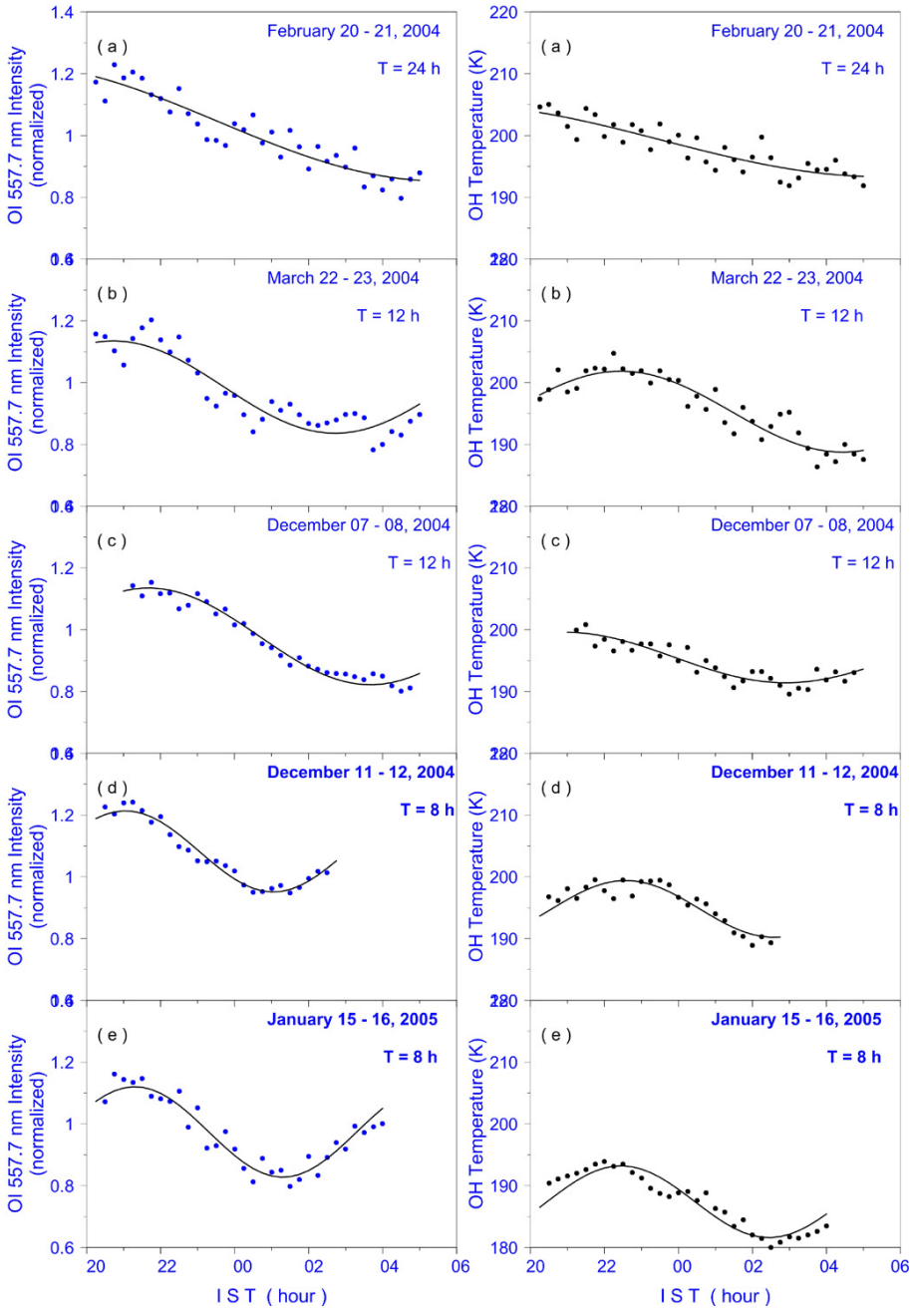

Fig. 5. Examples of tidal oscillations observed in OI 557.7 nm emission and OH temperature. The solid curves represent the sinusoidal least square fit (confidence level of 95 %) of the form $A\sin[(2\pi/T)(t-\phi)]$.

performed, and the averaged intensity and temperature is shown in Fig. 6 (the error bars indicate the range of variations observed at a particular time of the averaged dataset). Takahashi et al. (1998) and Buriti et al. (2001) believe that such an averaging removes the random short-period oscillations due to gravity waves and retains the coherent long period oscillations. Herein, it was noticed that the night-to-night variation of the phase of this 8 h feature was less than 0.6 h, and hence it can be safely assumed that the tidal feature was retained in the averaging process. A very clear tidal feature with a crest and trough is apparent in the averaged intensity and temperature variations during the month of January. A Lomb-Scargle analysis of this averaged intensity and temperature series was performed. It indicated that an 8.2 h and 8 h wave governs the averaged variation during January 2004 and January 2005, respectively; they are shown by the solid curves (least square fit based) in Fig. 6. Identical with earlier observation for the individual nights, a good

Table 2. Results of Lomb-Scargle analysis for tide-like oscillations ∼ monthly characterization.

Month	Campaign I (November 2003–April 2004)		Campaign II (December 2004–May 2005)	
	Harmonics observed in OH temperature dataset	Harmonics observed in OI 557.7 nm dataset	Harmonics observed in OH temperature dataset	Harmonics observed in OI 557.7 nm dataset
December	**12.2 h**, **9.6 h**	24.2 h, **12 h**, **9.8 h**	24.3 h, **12 h**, **9 h**	24.3 h, **12 h**, **8.8 h**
January	12 h, **8 h**	12 h, **8 h**	23.2 h, **7.9 h**	23.5 h, **8 h**
February	**24 h**, **12.2 h**, 8.2 h	**24 h**, **12 h**, 8 h	**11.7 h**, 7.6 h	**24.2 h**, **12.1 h**, 8 h
March	**23.5 h**, **11.9 h**	**24 h**, **12 h**	**24 h**, **12 h**, 8.4 h	**12.2 h**, 8.1 h
April	**23.4 h**, **12 h**, 8.1 h	**24 h**, **12 h**	–	–
May	–	–	**24.2 h**, **12 h**, 8.2 h	**24.2 h**, **12.1 h**, 8.1 h

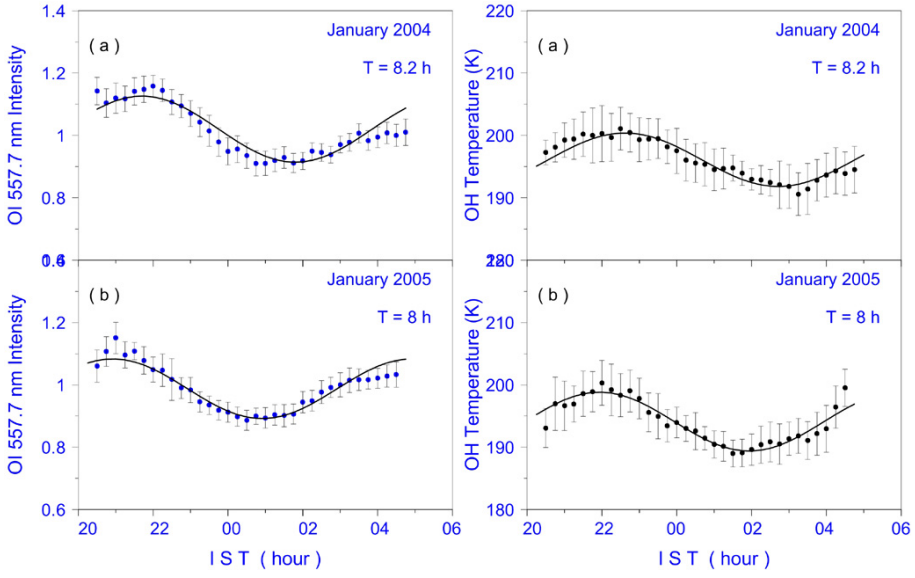

Fig. 6. Averaged variation of OI 557.7 intensity and OH temperature during January 2004 and January 2005. The error bars represent the standard deviation of the averaged values at a particular time, and the solid curves represent the sinusoidal least square terdiurnal fit (confidence level of 95 %) of the form $A\sin[(2\pi/T)(t-\phi)]$.

correspondence (well within the error bars) between the averaged variations and the forced terdiurnal harmonic fit can be observed. Based on this harmonic fitting, the characteristics of the assumed terdiurnal wave were estimated, and the results are presented in Table 3. A close agreement between the measurements (in terms of dominant harmonic, amplitude, vertical wavelength, and phase speed) during the two epochs can be seen, and this furthermore supports the inferences made on the terdiurnal tide during January. It is found that the terdiurnal tidal amplitudes are less than or comparable to that of diurnal and semidiurnal tides, a fact that can also be visualized in Fig. 5. This is the first report of terdiurnal tides observed in the nightglow measurements over the Indian subcontinent.

Many previous works have reported the observations of 8 h tide in the MLT region (for example, Glass and Fellons, 1975; Teitelbaum et al., 1989; Oznovich et al., 1995, 1997; Thayaparan, 1997; Taylor et al., 1999; Smith, 2000; Younger et al., 2002; Taori et al., 2005; Wu et al., 2005; Beldon et al., 2006; Jiang et al., 2009; Rao et al., 2011). Glass and Fellons (1975) and Teitelbaum et al. (1989) suggested that this wave can be interpreted both as the solar driven terdiurnal tide and as the result of nonlinear interaction between diurnal and semi-diurnal tides. Oznovich et al. (1995, 1997) observed the prominent terdiurnal oscillations in OH intensity and temperature over Eureka, Nunavut (80° N), Canada. Thayaparan (1997) reported the observations of 8 h tides in the MLT region using 2 MHz radar near London (43° N, 81° W), Canada. Taylor et al. (1999) combined the observations of Na Lidar and a CCD based OH temperature mapper to study the 8 h tides. Smith (2000) reported the latitudinal structure and seasonal variation of the terdiurnal tides using the wind observations of HRDI instrument on-board UARS. Younger et al. (2002) investigated the 8 h tidal phenomena

Table 3. Characteristics of the terdiurnal oscillation observed during January 2004 and January 2005.

Month	Periodicity (h)	Amplitude (K)	Vertical wavelength (km)	Phase speed ($m\,s^{-1}$)
January 2004	8.2	4.3	116	3.97
January 2005	8.0	4.7	100	3.47

over Esrange (68° N, 21° E), Sweden, using an all-sky VHF meteor radar. The authors found this 8 h tide to be a persistent feature of the Arctic mesosphere-lower thermosphere and interpreted it as a result of the nonlinear interaction between the 12- and 24-h tides. Later on, using a VHF meteor radar data collected between 1988 and 2004 over Castle Eaton (52.6° N, 2.2° W), Beldon et al. (2006) reported the constant presence of the 8 h tide at an altitude of 90–95 km. Taori et al. (2005) observed a persistent 8 h oscillation in the OH (6, 2) and O_2 (0, 1) nocturnal rotational temperatures – a proxy of atmospheric temperatures at altitudes of 87 and 94 km, respectively. The authors also noted an 8 h periodicity in simultaneously measured meteor radar wind data. Wu et al. (2005) noted the occurrence of 8 h oscillation in OH brightness and temperature, which they simultaneously measured using Fabry-Perot interferometer at Resolute (75° N). Jiang et al. (2009) studied the characteristics of 8 h tides in the MLT region using wind data from the meteor radar at a low latitude station in Maui (20.75° N). The authors found the 8 h tides to be a regular and distinct dynamical feature of the MLT region over Maui. Most recently, Rao et al. (2011) have reported the occurrence and variability of terdiurnal tides in the MLT region over Tiruneveli (8.7° N, 77.8° E), Koto Tabang (0.2° S, 100.3° E), and Pameungpeuk (7.4° S, 107.4° E) using meteor wind radar measurements. It is worthy to mention here that Tirunelveli is an equatorial station located within a distance of 9° from Kolhapur – the site of current study. As a matter of coincidence, these authors used the wind data between January 2003 and December 2007, which are included in the measurement epoch of current study (viz. November 2003 to April 2004 and December 2004 to May 2005). The authors subjected the hourly zonal and meridional wind data to a fast Fourier transform, and found a distinct terdiurnal peak (apart from diurnal and semidiurnal peaks) well above the gravity wave continuum. In their study, firstly the terdiurnal tidal amplitudes were less than the diurnal and semidiurnal ones, with the monthly mean value in the range of 1–10 $m\,s^{-1}$; and secondly the terdiurnal amplitude and phase was around 4 $m\,s^{-1}$ and 4–5 h, respectively, at 90 km over Tirunelveli during January. These authors concluded from their comprehensive study that the terdiurnal tide is a permanent feature of the equatorial MLT region, attributing their presence to firstly, the nonlinear interaction between diurnal and semidiurnal tides, and secondly, the interaction between gravity waves and diurnal tide.

3 Conclusions

Nightglow measurements of the atomic oxygen green line at 557.7 nm have been carried out at a low latitude station, Kolhapur (17° N), India, during November 2003 to April 2004 and December 2004 to May 2005. This report is the first to present the nocturnal behaviour of this emission feature over a prolonged period of time, spanning winter and spring during 2003–2005. Nocturnal behaviour of OI 557.7 nm intensity is marked by two types of equally occurring trends: firstly, the monotonic decreasing trend from beginning of the night to the dawn hours; and secondly, the decrease of intensity from pre-midnight to midnight hours, thereby attaining a minima around 01:00 h followed by the post-midnight increase. The observed nocturnal behaviour is in good agreement with the earlier reports. An analysis of the entire OI 557.7 nm intensity and OH temperature database indicates that the long period temporal variations are probably driven by a terdiurnal tide on most occasions, and OI 557.7 nm intensity variation leads that of OH temperature variation by less than an hour. These observations of terdiurnal tides from Kolhapur (16.8° N) are consistent with the recent report of terdiurnal tides in the meteor wind data from Tirunelveli (8.7° N) by Rao et al. (2011). On a few occasions, similar waves (having periodicity in the range of 2–3 h) were noted in OI 557.7 nm intensity and OH temperature series.

Acknowledgements. Nightglow measurements have been carried out at Kolhapur, India, under scientific collaboration between Indian Institute of Geomagnetism, Navi Mumbai and Shivaji University, Kolhapur. The funds for the research studies are being provided by Department of Science and Technology (DST), Govt. of India, New Delhi. Technical support received from P. T. Patil in nightglow observations is gratefully acknowledged.

The authors are grateful to the esteemed referees for evaluating the paper.

Topical Editor C. Jacobi thanks P. Muralikrishna and three other anonymous referees for their help in evaluating this paper.

References

Bates, D. R.: Excitation of 557.7 nm OI line in nightglow, Planet. Space Sci., 36, 883–889, 1988.

Bates, D. R.: Nightglow emissions from oxygen in the lower thermosphere, Planet. Space Sci., 40, 211–221, 1992.

Beldon, C. L., Muller, H. G., and Mitchell, N. J.: The 8-hour tide in the mesosphere and lower thermosphere over the UK, 1988–2004, J. Atmos. Solar-Terr. Phys., 68, 655–668, 2006.

Brasseur, G. and Solomon, S.: Aeronomy of the middle atmosphere: Chemistry and physics of the stratosphere and mesosphere, D. Reidel Publishing Co., 1984.

Brenton, J. G. and Silverman, S. M.: A study of the diurnal variations of the 5577 Å [OI] airglow emission at selected IGY stations, Planet. Space Sci., 18, 641–653, 1970.

Buriti, R. A., Takahashi, H., and Gobbi, D.: Temporal variation of the volume emission rates between OI5577 and O_2 (0, 1), Adv. Space Res., 27, 1159–1164, 2001.

Chiplonkar, M. W. and Tillu, A. D.: The F-layer component of the 5577 Å emission of the night airglow at Poona, Annales de Geophysique, 26, 213–222, 1970.

Clemesha, B. R., Takahashi, H., Batista, P. P., Sahai, Y., and Simonich, D. M.: The temperature dependence of airglow emissions from the upper mesosphere and lower thermosphere, Planet. Space Sci., 39, 1397–1404, 1991.

Cogger, L. L., Elphinstone, R. D., and Giers, D. H.: Wave characteristics obtained from OH rotational temperatures and 557.7 nm airglow intensities, J. Atmos. Terr. Phys., 50, 943–949, 1988.

Das, U. and Sinha, H. S. S.: Long-term variations in oxygen green line emission over Kiso, Japan, from ground photometric observations using continuous wavelet transform, J. Geophys. Res., 113, D19115, doi:10.1029/2007JD009516, 2008.

Fukuyama, K.: Airglow variations and dynamics in the lower thermosphere and upper mesosphere – 1: Diurnal variation and its seasonal dependency, J. Atmos. Terr. Phys., 38, 1279–1287, 1976.

Glass, M. and Fellons, J. I.: The eight-hourly (terdirunal) component of atmospheric tides, Space Research, XV, 191–197, Akademic-Verlag, Berlin, 1975.

Gobbi, D., Takahashi, H., Clemesha, B. R., and Batista, P. P.: Equatorial atomic oxygen profiles derived from rocket observations of OI 557.7 nm airglow emission, Planet. Space Sci., 40, 775–781, 1992.

Jiang, G., Xu, J., and Franke, S. J.: The 8-h tide in the mesosphere and lower thermosphere over Maui (20.75° N, 156.43° W), Ann. Geophys., 27, 1989–1999, doi:10.5194/angeo-27-1989-2009, 2009.

Kulkarni, P. V.: Rocket study of 5577-A O I emission at night over the magnetic equator, J. Geophys. Res., 81, 3740–3744, 1976.

Liu, G. and Shepherd, G. G.: Perturbed profiles of oxygen nightglow emissions as observed by WINDII on UARS, J. Atmos. Solar-Terr. Phys., 68, 1018–1028, 2006.

Liu, G., Shepherd, G. G., and Roble, R. G.: Seasonal variations of the nighttime O (^{1}S) and OH airglow emission rates at mid-to-high latitudes in the context of the large-scale circulation, J. Geophys. Res., 113, A06302, doi:10.1029/2007JA012854, 2008a.

Liu, G., Shepherd, G. G., and Tepley, C. A.: Variations of the tropical O (^{1}S) nightglow as observed with the Arecibo Observatory photometer and WINDII on UARS, J. Atmos. Solar-Terr. Phys., 70, 1309–1317, 2008b.

McDade, I. C. and Llewellyn, E. J.: The excitation of O (^{1}S) and O_2 bands in the nightglow – A brief review and preview, Canadian J. Phys., 64, 1626–1630, 1986.

Meriwether, J. W.: A review of the photochemistry of selected nightglow emissions from the mesopause, J. Geophys. Res., 94, 14629–14646, 1989.

Misawa, K. and Takeuchi, I.: Nightglow intensity variations in the O2(0-1) atmospheric band, the NaD lines, the OH(6-2) band, the yellow-green continuum at 5750 A and the oxygen green line, Annales de Geophysique, 38, 781–788, 1982.

Mukherjee, G. K.: The signature of short-period gravity waves imaged in the OI 557.7 nm and near infrared OH nightglow emissions over Panhala, J. Atmos. Solar-Terr. Phys., 65, 1329–1335, 2003.

Murtagh, D. P., Witt, G., Stegman, J., McDade, I. C., Llewellyn, E. J., Harris, F., and Greer, R. G. H.: An assessment of proposed O(^{1}S) and $O_2(b^1\Sigma_g^+)$ nightglow excitation parameters, Planet. Space Sci., 38, 43–53, 1990.

Oznovich, I., McEwen, D. J., and Sivjee, G. G.: Temperature and airglow brightness oscillations in the polar mesosphere and lower thermosphere, Planet. Space Sci., 43, 1121–1130, 1995.

Oznovich, I., Walterscheid, R. L., Sivjee, G. G., and McEwen, D. J.: On Krassovsky's ratio for terdiurnal hydroxyl oscillations in the winter polar mesopause, Planet. Space Sci., 45, 385–394, 1997.

Parihar, N. and Mukherjee, G. K.: Measurement of mesopause temperature from hydroxyl nightglow at Kolhapur (16.8° N, 74.2° E), India, Adv. Space Res., 41, 660–669, 2008.

Petitdidier, M. and Teitelbaum, H.: Lower thermosphere emissions and tides, Planet. Space Sci., 25, 711–721, 1977.

Petitdidier, M. and Teitelbaum, H.: O (^{1}S) excitation mechanism and atmospheric tides, Planet. Space Sci., 27, 1409–1419, 1979.

Rao, V. R. and Kulkarni, P. V.: Covariation of 6300 A and 5577 A emissions in tropical night airglow and the emission of 5577 A from the F-region, Annales de Geophysique, 30, 291–300, 1974.

Rao, N. V., Tsuda, T., Gurubaran, S., Miyoshi, Y., and Fujiwara, H.: On the occurrence and variability of the terdiurnal tide in the equatorial mesosphere and lower thermosphere and a comparison with the Kyushu-GCM, J. Geophys. Res., 116, D02117, doi:10.1029/2010JD014529, 2011.

Rayleigh, L.: The light of the night sky: Its intensity variations when analyzed by colour filters, Proc. R. Soc. London, Ser. A, 119, 117–137, 1924.

Rayleigh, L. and Jones, H. S.: The light of the night-sky: Analysis of the intensity variations at three stations, Proc. R. Soc. London, Ser. A, 151, 22–55, 1935.

Shepherd, G. G. and McLandress, C.: Southern hemisphere dynamics observed by WINDII: The wind imaging interferometer on the UARS mission, Adv. Space Res., 16, (5)53–(5)60, 1995.

Smith, A. K.: Structure of the terdiurnal tide at 95 km, Geophys. Res. Lett., 27, 177–180, 2000.

Smith, A. K.: Physics and chemistry of the mesopause region, J. Atmos. Solar-Terr. Phys., 66, 839–857, 2004.

Takahashi, H., Sahai, Y., Clemesha, B. R., Batista, P. P., and Teixeira, N. R.: Diurnal and seasonal variations of the OH (8, 3) airglow band and its correlation with OI 5577 Å, Planet. Space Sci., 25, 541–547, 1977.

Takahashi, H., Batista, P. P., Clemesha, B. R., Simonich, D. M., and Sahai, Y.: Correlations between OH, NaD and OI 5577 Å emissions in the airglow, Planet. Space Sci., 27, 801–807, 1979.

Takahashi, H., Batista, P. P., Sahai, Y., and Clemesha, B. R.: Atmospheric wave propagations in the mesopause region observed by the OH (8,3) band, NaD, O_2A(8645Å) band and OI 5577 Å nightglow emissions, Planet. Space Sci., 33, 381–384, 1985.

Takahashi, H., Sahai, Y., Clemesha, B. R., Simonich, D. M., Teixeira, N. R., Lobo, R. M., and Eras, A.: Equatorial mesospheric and F-region airglow emissions observed from latitude 4° south, Planet. Space Sci., 37, 649–655, 1989.

Takahashi, H., Gobbi, D., Batista, P. P., Melo, S. M. L., Teixeira, N. R., and Buriti, R. A.: Dynamical influence on the equatorial airglow observed from the south american sector, Adv. Space Res., 21, 817–825, 1998.

Taori, A., Sridharan, R., Chakrabarty, D., Modi, N. K., and Narayanan, R.: Significant upper thermospheric contribution to the O (^{1}S) 557.7 nm dayglow emission: first ground based evidence, J. Atmos. Solar-Terr. Phys., 65, 121–128, 2003.

Taori, A., Taylor, M. J., and Franke, S.: Terdiurnal wave signatures in the upper mesospheric temperature and their association with the wind fields at low latitudes (20° N), J. Geophys. Res., 110, D09S06, doi:10.1029/2004JD004564, 2005.

Taylor, M. J., Pendleton Jr., W. R., Gardner, C. S., and States, R. J.: Comparison of terdiurnal tidal oscillations in mesospheric OH rotational temperature and Na lidar temperature measurements at mid-latitudes for fall/spring conditions, Earth, Planets Space, 51, 877–885, 1999.

Teitelbaum, H., Vial, F., Manson, A. H., Giraldez, R., and Masseboeuf, M.: Nonlinear interaction between the diurnal and semidiurnal tides: Terdiurnal and diurnal secondary waves, J. Atmos. Solar-Terr. Phys., 51, 609–616, 1989.

Thayaparan, T.: The terdiurnal tide in the mesosphere and lower thermosphere over London, Canada (43° N, 81° W), J. Geophys. Res., 102, 21695–21708, 1997.

Wiens, R. H., Taylor, M. J., Zhang, S. P., and Shepherd, G. G.: Coupled Longitudinal and Tidal Variations of Equatorial Nightglow O (^{1}S) Zenith Emission Rates from WINDII and Christmas Island Data, Adv. Space Res., 24, 1577–1582, 1999.

Wu, Q., Mitchell, N. J., Killeen, T. L., Solomon, S. C., and Younger, P. T.: A high-latitude 8-hour wave in the mesosphere and lower thermosphere, J. Geophys. Res., 110, A09301, doi:10.1029/2005JA011024, 2005.

Yee, J-. H. and Abreu, V. J.: Mesospheric 5577 Å green line and atmospheric motions-Atmosphere explorer satellite observations, Planet. Space Sci., 35, 1389–1395, 1987.

Yee, J-. H., Crowley, G., Roble, R. G., Skinner, W. R., Burrage, M. D., and Hays, P. B.: Global simulations and observations of O(^{1}S), O_2($^1\Sigma$) and OH mesospheric nightglow emissions, J. Geophys. Res., 102, 19949–19968, 1997.

Younger, P. T., Pancheva, D., Middleton, H. R., and Mitchell, N. J.: The 8-hour tide in the Arctic mesosphere and lower thermosphere, J. Geophys. Res. (Space Physics), 107, SIA 2-1, 1420, 2002.

Zhang, S. P. and Shepherd, G. G.: The influence of the diurnal tide on the O(^{1}S) and OH emission rates observed by WINDII on UARS, Geophys. Res. Lett., 26, 529–532, 1999.

Zhang, S. P., Wiens, R. H., Solheim, B. H., and Shepherd, G. G.: Nightglow zenith emission rate variations in O(^{1}S) at low latitudes from wind imaging interferometer (WINDII) observations, J. Geophys. Res., 103, 6251–6260, 1998.